Regenerative Therapy 20 (2022) 138–146

Contents lists available at ScienceDirect

Regenerative Therapy

journal homepage: http://www.elsevier.com/locate/reth

Original Article

Circ_ROBO2/miR-186-5p/TRIM14 axis regulates oxidized low-density lipoprotein-induced cardiac microvascular endothelial cell injury

Qinghu Ye [a], Changlin Ju [b], Zhou Ye [a], Jiaqiong Tong [a, *]

[a] Department of Cardiology, The First People's Hospital of Hangzhou Lin'an District, Ward 1, Hangzhou 311300, China
[b] Department of Cardiovascular Medicine, The First Affiliated Hospital of Wannan Medical College, Wuhu 241000, China

ARTICLE INFO

Article history:
Received 8 November 2021
Received in revised form
23 February 2022
Accepted 14 April 2022

Keywords:
Coronary artery disease
Oxidized low-density lipoprotein
Circ_ROBO2
miR-186-5p
TRIM14

ABSTRACT

Background: Coronary artery disease (CAD) is one of the main risks of death, which is mainly caused by coronary arteries arteriosclerosis. Circular RNAs (circRNAs) have shown important regulatory roles in cardiovascular diseases. We amid to explore the role of circ_ROBO2 in CAD.
Methods: Cardiac microvascular endothelial cells (CMECs) stimulated by oxidized low-density lipoprotein (ox-LDL) were served as the cellular model of CAD. Real-time quantitative polymerase chain reaction (RT-qPCR) and western blot assay were performed to detect RNA levels and protein levels, respectively. Cell proliferation was assessed by 5-ethynyl-2′-deoxyuridine (EdU) assay and Cell Counting Kit-8 (CCK-8) assay. Flow cytometry was employed for measuring cell apoptosis. Matrigel tube formation assay was used to evaluate angiogenesis ability. The intermolecular interaction was predicted by bioinformatics analysis and verified by dual-luciferase reporter and RNA-pull down assays.
Results: The expression of circ_ROBO2 was upregulated in CAD patients and ox-LDL-induced CMECs. Treatment of ox-LDL suppressed cell proliferation and angiogenic ability as well as promoted the apoptosis of CMECs partly by upregulating circ_ROBO2. MicroRNA-186-5p (miR-186-5p) was identified as a target of circ_ROBO2, and circ_ROBO2 knockdown attenuated ox-LDL-induced damage in CMECs by sponging miR-186-5p. Tripartite motif containing 14 (TRIM14) acted as a target of miR-186-5p, and TRIM14 overexpression alleviated miR-186-5p-mediated inhibitory effect on ox-LDL-induced injury in CMECs. Circ_ROBO2 positively regulated TRIM14 expression by sponging miR-186-5p.
Conclusion: Circ_ROBO2 played a promoting role in ox-LDL-induced CMECs injury by sponging miR-186-5p and regulating TRIM14, providing a promising treatment strategy for CAD.

1. Introduction

Coronary artery disease (CAD) is a common cardiovascular disease and is one of the main threats to human health worldwide [1,2]. CAD is characterized with coronary arteries arteriosclerosis, which is the main cause of sudden cardiac death [3]. The current treatment methods for CAD are mainly coronary artery bypass surgery and percutaneous coronary intervention [4]. However, CAD patients still had a worse prognosis with high mortality due to its complicated pathogenesis. Oxidized low-density lipoprotein (ox-LDL) has been reported to be implicated in the progression of atherosclerosis [5]. Thus, ox-LDL plays a critical role in cardiovascular diseases. Previous studies showed that ox-LDL-induced cardiac microvascular endothelial cells (CMECs) injury was used to establish CAD cell model [6]. Therefore, searching possible molecular targets to prevent related cell injury may be an effective method for CAD treatment.

Circular RNAs (circRNAs), a novel type of non-coding RNAs (ncRNAs), can form covalent closed-loop configurations, lacking 5′-end cap and 3′-end poly A tail [7]. Due to the closed-loop structures, circRNAs are more stable and not easily degraded by RNases [8]. Accumulating studies have confirmed the critical importance of circRNAs in human diseases in the past few decades [9,10]. In addition, some circRNAs have been identified to play pivotal roles in atherosclerosis [11,12]. Moreover, circ_0004104 was upregulated

* Corresponding author. Department of Cardiology, The First People's Hospital of Hangzhou Lin'an District, No. 548, Yijin Street, Ward 1, Jincheng Neighborhood, Lin'an District, Hangzhou 311300, China
E-mail address: tjq2566@163.com (J. Tong).
Peer review under responsibility of the Japanese Society for Regenerative Medicine.

https://doi.org/10.1016/j.reth.2022.04.005

in patients with CAD and its knockdown alleviated ox-LDL-induced vascular endothelial cell injury [13]. A previous report showed that circRNA roundabout guidance receptor 2 (circ_ROBO2; also known as circ_0124644) was upregulated in CAD patients [14], implicating that circ_ROBO2 might be related to CAD development. Therefore, the role and regulatory mechanism of circ_ROBO2 in CAD were explored.

Emerging evidence has shown that most circRNAs are located in the cytoplasm that can function as competitive endogenous RNAs (ceRNAs) or sponges/decoys for microRNAs (miRNAs) to combine with miRNAs, leading to the reduction of miRNA molecules and preventing the degradation of messenger RNAs targeted by these miRNAs [15,16]. MiRNAs, another kind of ncRNAs, bind to 3′UTR of target mRNAs to reversely modulate gene expression [17]. MiRNAs can act as important regulators in many diseases, including cardiovascular diseases [18,19]. MiR-186-5p was reported to play a critical role in cardiovascular diseases [20]. Moreover, a recent study indicated that tripartite motif containing 14 (TRIM14) was involved in the progression of atherosclerosis [21]. Coincidently, we first found that circ_ROBO2 and TRIM14 shared the complementary binding sites for miR-186-5p using bioinformatics tools, which prompted us to establish a circ_ROBO2/miR-186-5p/TRIM14 regulatory network.

In this work, we measured circ_ROBO2 expression in CAD patients and CAD cell model. Then we studied the impact of circ_ROBO2 on proliferation, apoptosis and angiogenesis in OA cell model. By mechanism study, we predicted and validated that circ_ROBO2 could modulate TRIM14 expression via sponging miR-186-5p.

2. Materials and methods

2.1. Clinical sample collection

Blood samples were collected from CAD patients (N = 23) without any therapy and healthy volunteers (N = 31) at the First People's Hospital of Hangzhou Lin'an District. The experiment was performed with approval of the ethics committee of the First People's Hospital of Hangzhou Lin'an District, and all participants signed the informed consents before enrolling in the study. Blood samples was then centrifuged (10 min, 3000 rpm) to extract serum samples.

2.2. Cell culture

Human CMECs were commercially provided by Procell (Wuhan, China) cultured in Dulbecco's modified eagle medium (DMEM; Invitrogen, Carlsbad, CA, USA) added with 10% fetal bovine serum (FBS; Invitrogen) under standard conditions (5% CO2, 37 °C). CMECs were exposed to ox-LDL (100 μg/mL; Solarbio, Beijing, China) for 24 h to construct CAD model *in vitro*.

2.3. Cell transfection

Short hairpin RNA targeting circ_ROBO2 (circ_ROBO2) and matched control (sh-NC), mimic or inhibitor of miR-186-5p (miR-186-5p or anti-miR-186-5p) and matched control (miR-NC or anti-miR-NC), TRIM14-overexpressing plasmid (TRIM14) and empty vector (pcDNA) were commercially provided by RiboBio (Guangzhou, China). CMECs were transfected with plasmids or/and oligonucleotides using Lipofectamine 3000 (Invitrogen, Carlsbad, CA, USA). After transfection for 48 h, the cells were harvested to perform function experiments.

2.4. Real-time quantitative polymerase chain reaction (RT-qPCR)

Total RNA was isolated utilizing TRIzol (Invitrogen). Next, the isolated RNA was reversed into cDNA with PrimeScript RT Master Mix (for mRNA and circRNA; PrimeScript RT Master Mix) and miScript II RT kit (for miRNA; Invitrogen). Next, RT-qPCR reaction was manipulated using the SYBR Green Master Mix (Roche, Shanghai, China) on Bio-Rad CFX96 system (Bio-Rad, Hercules, CA, USA). Relative abundance of circ_ROBO2, ROBO2, miR-186-5p and TRIM14 was analyzed using the $2^{-\Delta\Delta Ct}$ method. U6 (for miR-186-5p) or GAPDH (for circ_ROBO2, ROBO2 and TRIM14) was acted as the internal reference. Primer sequences were exhibited in Table 1.

2.5. Subcellular fractionation location

PARIS™ Kit (Invitrogen) was used to isolate the fractions of cytoplasmic and nuclear. RNA samples derived different fractions were used for RT-qPCR analysis. U6 acted as a nucleus control and GAPDH acted as a cytoplasm control.

2.6. Cyclization validation

To verify the closed-loop structure of circ_ROBO2, RNA samples were treated with or without RNase R (BioVision, Mipitas, CA, USA) for half an hour at 37 °C. RNA levels were examined via RT-qPCR.

To suppress the transcription, cells were exposed to Actinomycin D (transcription inhibitor; Seebio, Shanghai, China), and RT-qPCR was used to examine RNA levels at specific time points.

2.7. Cell proliferation assays

To test cell proliferation and DNA synthesis, 5-ethynyl-2′-deoxyuridine (EdU) assay was conducted with the use of EdU Cell Proliferation Kit (Beyotime, Jiangsu, China). Briefly, cells were added into the 24-well plates. After treatment, cells were incubated with EdU (10 μM) for 2 h. Next, 4% paraformaldehyde was used to fix EdU labeled cells. After that, we used 0.5% TritonX-100 to permeabilize cells, followed by incubation with Click Additive solution for 0.5 h in a darkness. DAPI was used to stain cell nucleic. Finally, EdU-positive cells were observed using fluorescence microscope (Leica, Wetzlar, Germany).

For Cell Counting Kit-8 (CCK-8) assay, CMECs were inoculated into a 96-well plate. At specific time points, CCK-8 reagent (10 μL; Beyotime) was placed into each well. 4 h post addition, the record of absorbance was carried out using the microplate reader (Bio-Rad) at 450 nm to detect cell viability.

2.8. Western blot assay

The lysis of proteins was administered by RIPA lysis buffer (Solarbio). After quantification of total protein, protein samples

Table 1
Primers sequences used for RT-qPCR.

Name	Primers (5′-3′)	
circ_ROBO2 (hsa_circ_0124644)	Forward	AGAAGTCAGAATACAGCAGG
	Reverse	GGTGAGATACAAGTGAAAAT
ROBO2	Forward	TCTTCGTTTTGATGCTCTTCCTC
	Reverse	GTCCTTGTCAGTCTCCACTCGCT
TRIM14	Forward	GCGTGGCTGAGCTCTTCTGTC
	Reverse	TGTGCTGCTGCTTCTTGATTG
miR-186-5p	Forward	GTATGACAAAGAATTCTCCT
	Reverse	TGGTGTCGTGGAGTCGT
GAPDH	Forward	AAGGCTGTGGGCAAGGTCATC
	Reverse	GCGTCAAAGGTGGAGGAGTGG
U6	Forward	CTCGCTTCGGCAGCACATA
	Reverse	CGAATTTGCGTGTCATCCT

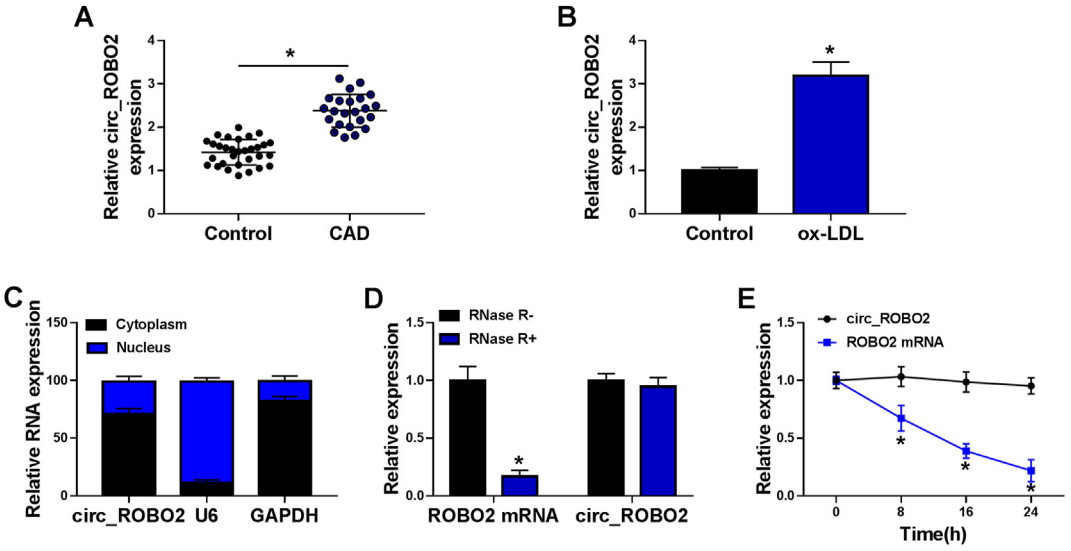

Fig. 1. Circ_ROBO2 was overexpressed in serum of CAD patients and ox-LDL-treated CMECs. (A) RT-qPCR was applied to measure the level of circ_ROBO2 in serum samples of CAD patients and healthy controls. (B) The expression of circ_ROBO2 was detected by RT-qPCR in CMECs treated with or without ox-LDL. (C) The expression of circ_ROBO2 was tested in nuclear and cytoplasm fractions. (D) RT-qPCR was carried out to examine the levels of circ_ROBO2 and ROBO2 mRNA with or without RNase R digestion. (E) Circ_ROBO2 and ROBO2 mRNA levels were examined by RT-qPCR after treatment with Actinomycin D. *$P < 0.05$.

(about 30 μg/lane) were separated using SDS-PAGE, followed by transferring onto PVDF membranes (Bio-Rad). After sealing with 5% non-fat milk (Beyotime), the proteins on the membranes were combined with primary antibodies for 12–16 h at 4 °C. After incubation with corresponding secondary antibody for 1–2 h (1:5000, ab205718, Abcam, Cambridge, UK), the ECL Substrate Kit (Abcam) was used to examine the conjugated signals. The primary antibodies contained proliferating cell nuclear antigen (PCNA; 1:500, ab18197, Abcam), Bcl-2 (1:2000, ab196495, Abcam), Bax (1:2000, ab53154, Abcam), TRIM14 (SAB1410027, Sigma, St. Louis, MO, USA), and GAPDH (1:2000, ab9485, Abcam).

2.9. Flow cytometry

CMECs were centrifuged and harvested, followed by resuspending in binding buffer (0.4 mL) and staining with Annexin V-FITC and PI (Sangon Biotech, Shanghai, China). Reacting for 0.5 h, flow cytometer (BD Biosciences, San Jose, CA, USA) was applied for detecting apoptotic cells.

2.10. Matrigel tube formation assay

Cell angiogenic ability was evaluated by Matrigel tube formation assay. In brief, 96-well plates were pre-coated with Matrigel (BD Biosciences). Then CMECs were plated onto the plates. After culturing for 48 h, tube images were captured using a microscope (Leica). The length of each tube was measured using Image J software with the Angiogenesis Analyzer plugin. The tube length in three random fields from each well was calculated to determine the average length.

2.11. Dual-luciferase reporter assay

Circinteractome (https://circinteractome.nia.nih.gov/) was applied to predict the target miRNAs for circ_ROBO2, starBase (http://starbase.sysu.edu.cn/) was employed to predict the target mRNAs for miR-186-5p. The fragments of circ_ROBO2 or TRIM14 3′UTR including the miR-186-5p-binding sequence were amplified and cloned into pmirGLO vector (YouBia, Changsha, China) to generate wild-type reporter vectors (circ_ROBO2-WT and TRIM14-WT). Meanwhile, mutated reporter vectors (circ_ROBO2-MUT and TRIM14-MUT) without miR-186-5p binding sites were generated as above described. Thereafter, miR-186-5p/miR-NC and the constructed reporter vector were co-transfected into CMECs. Dual Luciferase Reporter Gene Assay Kit (LMAI Bio, Shanghai, China) was utilized to analyze the luciferase activities after 48 h co-transfection.

2.12. RNA pull-down assay

Biotin-labeled negative control (Bio-NC), Biotin-labeled wild-type circ_ROBO2 or TRIM14 (circ_ROBO2-WT or TRIM14-WT) and Biotin-labeled mutant circ_ROBO2 or TRIM14 (circ_ROBO2-MUT or TRIM14-MUT) were obtained from RiboBio and individually transfected into CMECs. 48 h later, cell lysates were incubated with the streptavidin magnetic beads (Invitrogen) for the co-immunoprecipitation. At last, miR-186-5p enrichment was tested via RT-qPCR after RNA isolation from magnetic beads.

2.13. Statistical analysis

The data were displayed as mean ± standard deviation. All experiments were repeated for three times experiments. Statistical analysis was performed by GraphPad Prism 6.0 software (GraphPad Prism, San Diego, CA, USA). The comparisons between two groups were estimated by Student's *t*-test, while one-way analysis of variance (ANOVA) was used to compare difference among multiple groups (more than two groups). Pearson's correlation coefficient was used to detect the correlations among circ_ROBO2, miR-186-5p, and TRIM14 in serum of CAD patients. A significant difference was represented when $P < 0.05$.

3. Results

3.1. Circ_ROBO2 expression was upregulated in serum of CAD patients and CMECs treated with ox-LDL

The expression of circ_ROBO2 was detected by RT-qPCR in serum samples of CAD patients and healthy controls. The results

Table 2
Relationship between circ_ROBO2 expression and clinical characteristics of CAD patients.

	Circ_ROBO2 expression (N = 23)		
Clinical characteristics	High (N = 11)	Low (N = 12)	P value
Age (≤65 years)	5 (45.5%)	7 (58.3%)	0.537
Sex, male (%)	6 (54.5%)	6 (50%)	0.827
Body mass index (≤27)	7 (63.6%)	6 (50%)	0.510
Medical history of hypertension, n (%)	4 (36.4%)	5 (41.7%)	0.795
Medical history of dyslipidemia, n (%)	7 (63.6%)	6 (50%)	0.510

showed that circ_ROBO2 was upregulated in the serum of patients with CAD relative to healthy controls (Fig. 1A). Moreover, the relationship between circ_ROBO2 expression and clinical characteristics of CAD patients was analyzed. There were no significant differences in age, sex, body mass index, medical history of hypertension, and medical history of dyslipidemia between the low circ_ROBO2 expression group and high expression group (Table 2). Moreover, an increase expression of circ_ROBO2 was observed in CMECs exposed to ox-LDL compared with the control cells (Fig. 1B). Next, we explored the localization of circ_ROBO2 in CMECs cells. We found that circ_ROBO2 was mainly located in the cytoplasm (Fig. 1C). In general, RNase R can digest linear RNA but not circRNA. As expected, circ_ROBO2 was resistant to RNase R compared to its linear counterpart ROBO2 (Fig. 1D), indicating that circ_ROBO2 was a circRNA. The expression of circ_ROBO2 was almost unaffected with the treatment of transcriptional inhibitor Actinomycin D (Fig.

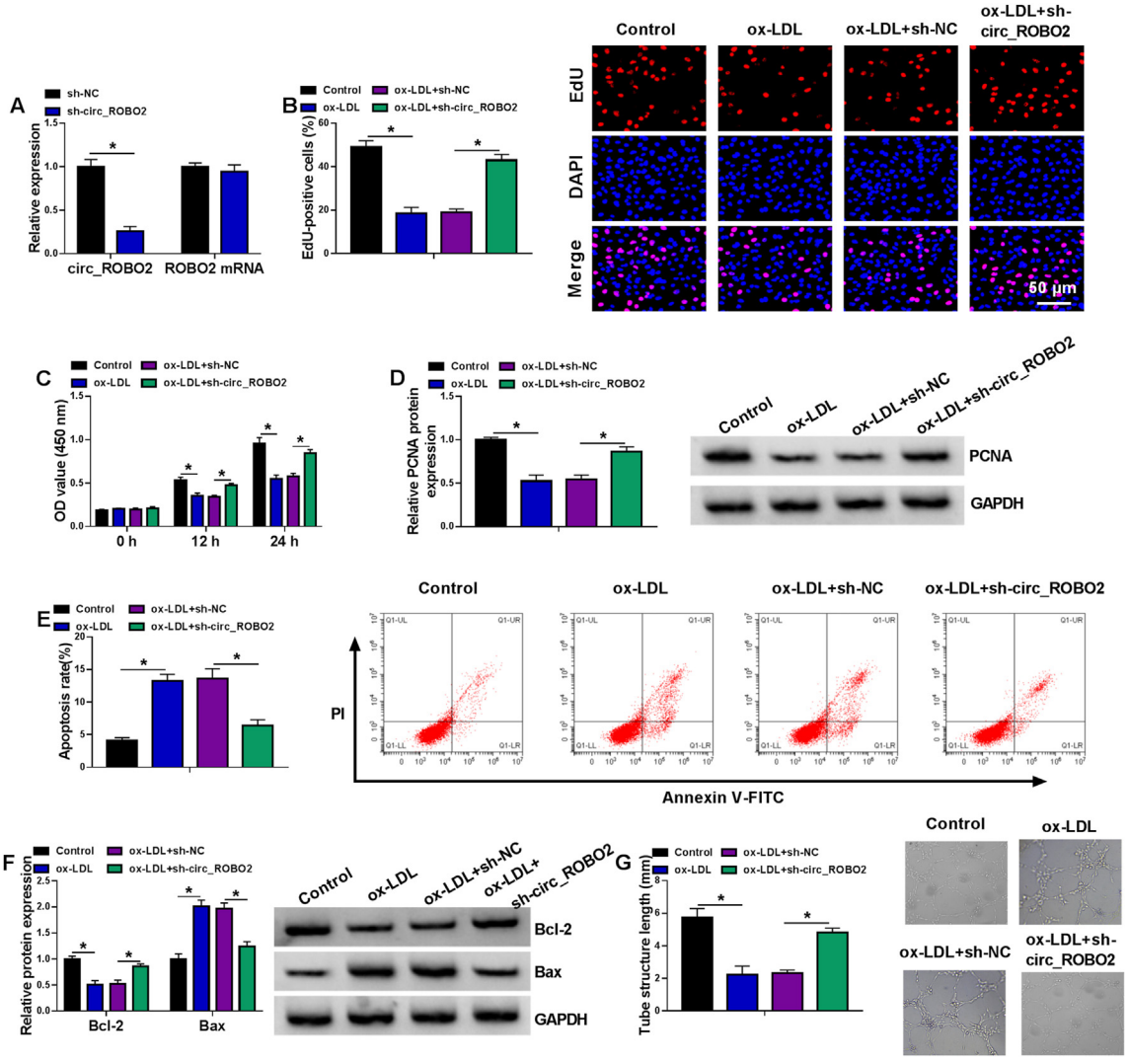

Fig. 2. Circ_ROBO2 knockdown alleviated ox-LDL-induced dysfunction in CMECs. (A) RT-qPCR was performed to evaluate the interference efficiency of sh-circ_ROBO2 in CMECs. (B–G) CMECs were divided into four groups: Control, ox-LDL, ox-LDL + sh-NC, and ox-LDL + sh-circ_ROBO2. (B) DNA synthesis was determined using an EdU assay. (C) Cell viability was assessed using CCK-8 assay. (D) The protein level of PCNA was detected by western blot assay. (E) The percentage of apoptotic CMECs was assessed by flow cytometry analysis. (F) The protein levels of Bcl-2 and Bax were analyzed by western blot assay. (G) Cell angiogenic ability was assessed by Matrigel tube formation assay. *$P < 0.05$.

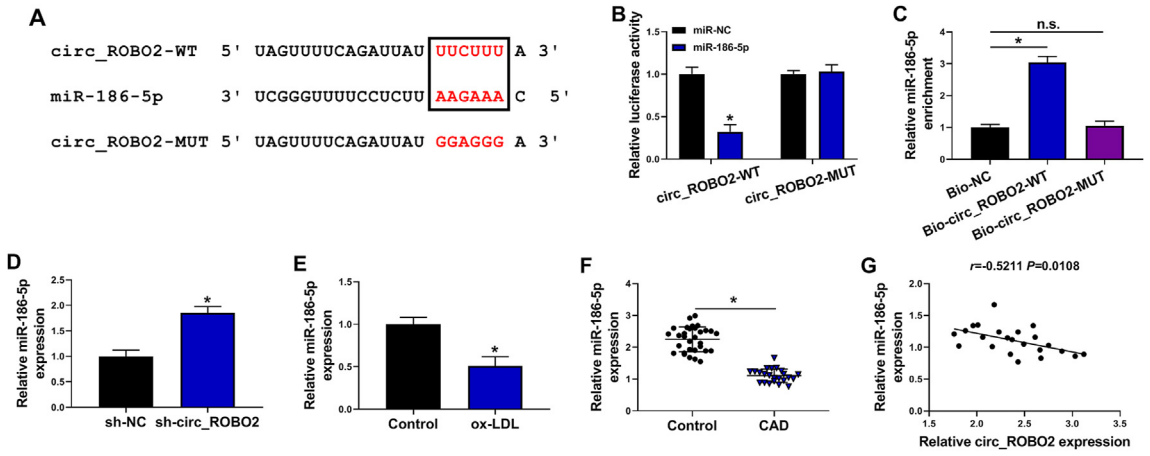

Fig. 3. MiR-186-5p was a direct target of circ_ROBO2. (A) The binding sites of circ_ROBO2 and miR-186-5p were predicted by circinteractome. (B and C) Dual-luciferase reporter assay and RNA-pull down assay were performed to verify the target relationship between circ_ROBO2 and miR-186-5p. (D) The expression of miR-186-5p was detected by RT-qPCR in CMECs transfected with sh-NC or sh-circ_ROBO2. (E) The expression of miR-186-5p was measured by RT-qPCR in CMECs treated with or without ox-LDL. (F) The level of miR-186-5p was detected by RT-qPCR in serum samples of CAD patients and healthy controls. (G) The correlation between circ_ROBO2 and miR-186-5p in serum samples of CAD patients was analyzed. $*P < 0.05$.

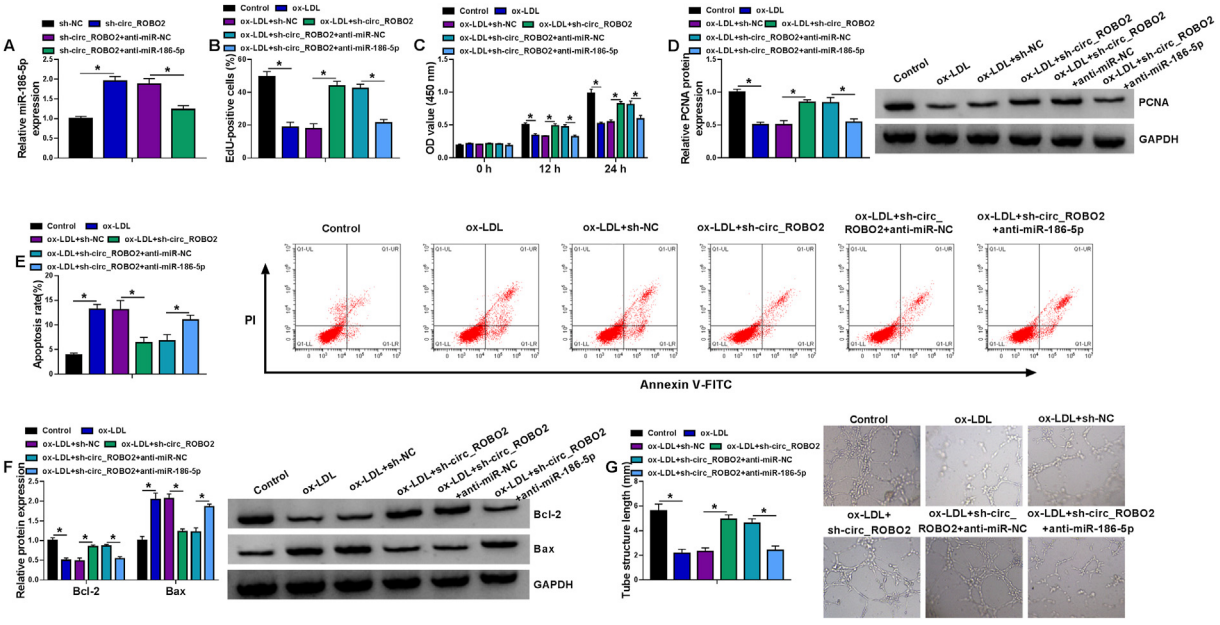

Fig. 4. Circ_ROBO2 downregulation weakened ox-LDL-induced dysfunction in CMECs via sponging miR-186-5p. (A) The expression of miR-186-5p was measured by RT-qPCR in CMECs transfected with sh-NC, sh-circ_ROBO2, sh-circ_ROBO2 + anti-miR-NC, or sh-circ_ROBO2 + anti-miR-186-5p. (B–G) CMECs were divided into six groups: Control, ox-LDL, ox-LDL + sh-NC, ox-LDL + sh-circ_ROBO2, ox-LDL + sh-circ_ROBO2 + anti-miR-NC, and ox-LDL + sh-circ_ROBO2 + anti-miR-186-5p. (B) EdU assay was used to detect DNA synthesis. (C) CCK-8 assay was applied to analyze cell viability. (D) PCNA protein level was determined by western blot assay. (E) Flow cytometry was carried out to analyze cell apoptosis rate. (F) Bcl-2 and Bax protein levels were examined by western blot assay. (G) Matrigel tube formation assay was used to examine angiogenesis. $*P < 0.05$.

1E), indicating that circ_ROBO2 was more stable than its linear form (ROBO2) in CMECs. These results indicated that circ_ROBO2 was an upregulated circRNA in CAD.

3.2. Knockdown of circ_ROBO2 attenuated ox-LDL-induced dysfunction in CMECs

Transfection efficiency was confirmed by RT-qPCR. Transfection of sh-circ_ROBO2 reduced circ_ROBO2 expression, but did not affect ROBO2 mRNA expression (Fig. 2A), indicating that transfection of sh-circ_ROBO2 was successful. Next, we explored the role of circ_ROBO2 in ox-LDL-induced CMECs. Cell proliferation was assessed by EdU and CCK-8 assays. We found that ox-LDL treatment suppressed CMEC proliferation via inhibiting DNA synthesis and cell viability, while knockdown of circ_ROBO2 abated the inhibitory effect of ox-LDL on proliferation in CMECs (Fig. 2B and C). Western blot assay showed that PCNA (a growth-promoting protein) protein expression was decreased by ox-LDL treatment, which was mitigated by circ_ROBO2 interference (Fig. 2D). Flow cytometry showed that ox-LDL exposure induced apoptosis in CMECs, and this effect was abated by circ_ROBO2 knockdown (Fig. 2E). Consistent with flow cytometry, ox-LDL treatment decreased the protein expression of Bcl-2 (anti-apoptotic molecule) and increased the protein expression of Bax (pro-apoptotic molecule) in CMECs, which was reversed by circ_ROBO2 downregulation (Fig. 2F). Cell angiogenic ability was inhibited by treatment of ox-LDL in CMECs, whereas this

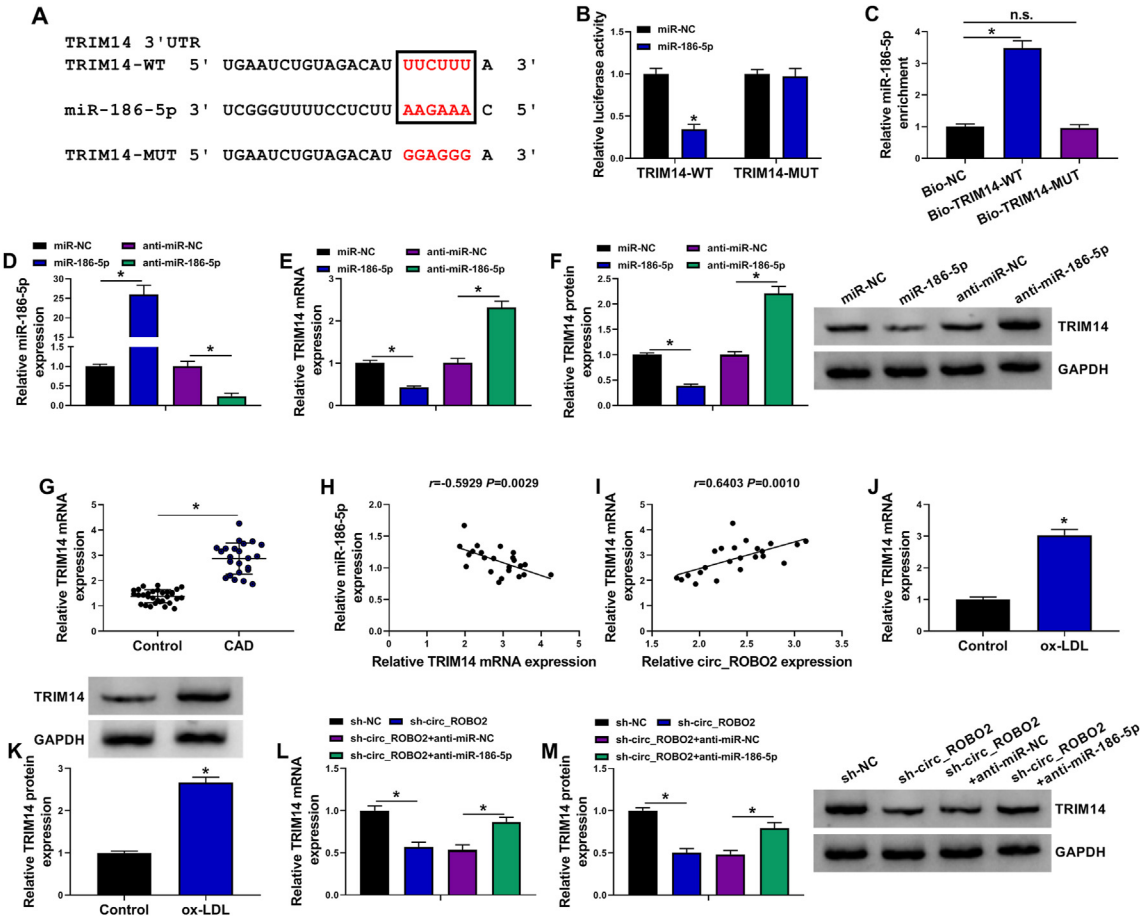

Fig. 5. TRIM14 was a direct target of miR-186-5p. (A) The interacted sites between miR-186-5p and TRIM14 3′UTR were predicted by starBase. (B and C) The binding relationship between miR-186-5p and TRIM14 were validated by dual-luciferase reporter assay and RNA-pull down assay. (D) The interference efficiency of anti-miR-186-5p and overexpression efficiency of miR-186-5p were tested by RT-qPCR. (E and F) TRIM14 mRNA and protein expression were analyzed by RT-qPCR and western blot assay in CMECs transfected with miR-NC, miR-186-5p, anti-miR-NC, or anti-miR-186-5p. (G) TRIM14 mRNA expression was tested by RT-qPCR in serum samples of CAD patients and healthy controls. (H and I) The correlation between TRIM14 and miR-186-5p or circ_ROBO2 was analyzed in CAD patient serum. (J and K) The mRNA and protein levels of TRIM14 were detected by RT-qPCR and western blot assay in CMECs treated with or without ox-LDL. (L and M) TRIM14 mRNA and protein levels were assessed by RT-qPCR and western blot assay in CMECs transfected with sh-NC, sh-circ_ROBO2, sh-circ_ROBO2 + anti-miR-NC, or sh-circ_ROBO2 + anti-miR-186-5p. *$P < 0.05$.

inhibitory effect was counteracted by transfection of sh-circ_ROBO2 (Fig. 2G). Collectively, ox-LDL-induced injury in CMECs was partly based on the upregulating circ_ROBO2.

3.3. Circ_ROBO2 acted as a sponge for miR-186-5p

Interestingly, circRNAs has been reported to act as molecular sponges of miRNAs in the cytoplasm of cells [22]. Given that circ_ROBO2 was dominantly located in cytoplasm, we supposed that circ_ROBO2 might act as a miRNA sponge. As expected, there were complementary binding sites between circ_ROBO2 and miR-186-5p (Fig. 3A), indicating that circ_ROBO2 might act as a sponge of miR-186-5p. Dual-luciferase reporter assay and RNA pull-down were executed to verify the interaction between circ_ROBO2 and miR-186-5p. The results revealed that miR-186-5p overexpression reduced the luciferase intensity of circ_ROBO2-WT, while the apparent change of circ_ROBO2-MUT group was unobserved (Fig. 3B). RNA pull-down assay showed that Bio-circ_ROBO2-WT led to higher miR-186-5p enrichment than treatment of Bio-circ_ROBO2-MUT or Bio-NC in CMECs (Fig. 3C). Next, we explored the effect of circ_ROBO2 on miR-186-5p expression. As presented Fig. 3D, the expression of miR-186-5p was increased by downregulating circ_ROBO2 in CMECs. Moreover, treatment of ox-LDL downregulated the expression of miR-186-5p in CMECs (Fig. 3E). Similarly, miR-186-5p expression was reduced in serum samples of CAD patients compared with healthy volunteers (Fig. 3F). Next, the correlation between miR-186-5p and circ_ROBO2 was analyzed in serum samples of CAD patients. A negative correlation between miR-186-5p and circ_ROBO2 was observed serum samples of CAD patients (Fig. 3G). Overall, miR-186-5p was a direct target of circ_ROBO2.

3.4. Circ_ROBO2 silencing attenuated ox-LDL-induced injury in CMECs partly through upregulating miR-186-5p

To investigate whether the regulatory effect of circ_ROBO2 was associated with miR-186-5p, we performed rescue experiments. Knockdown of circ_ROBO2 increased miR-186-5p expression, which was weakened by transfection of anti-miR-186-5p in CMECs (Fig. 4A). MiR-186-5p inhibition could abolish the promotive effects of sh-circ_ROBO2 on DNA synthesis, cell viability, and PCNA protein expression in ox-LDL-treated CMECs (Fig. 4B–D), indicating that the promoting effect of circ_ROBO2 knockdown was reversed by inhibiting miR-186-5p. Moreover, the inhibitory effect of circ_ROBO2 downregulation on apoptosis was abrogated by miR-186-5p inhibition in ox-LDL-treated CMECs (Fig. 4E). Consistently, the increase of Bcl-2 protein expression and decrease of Bax protein

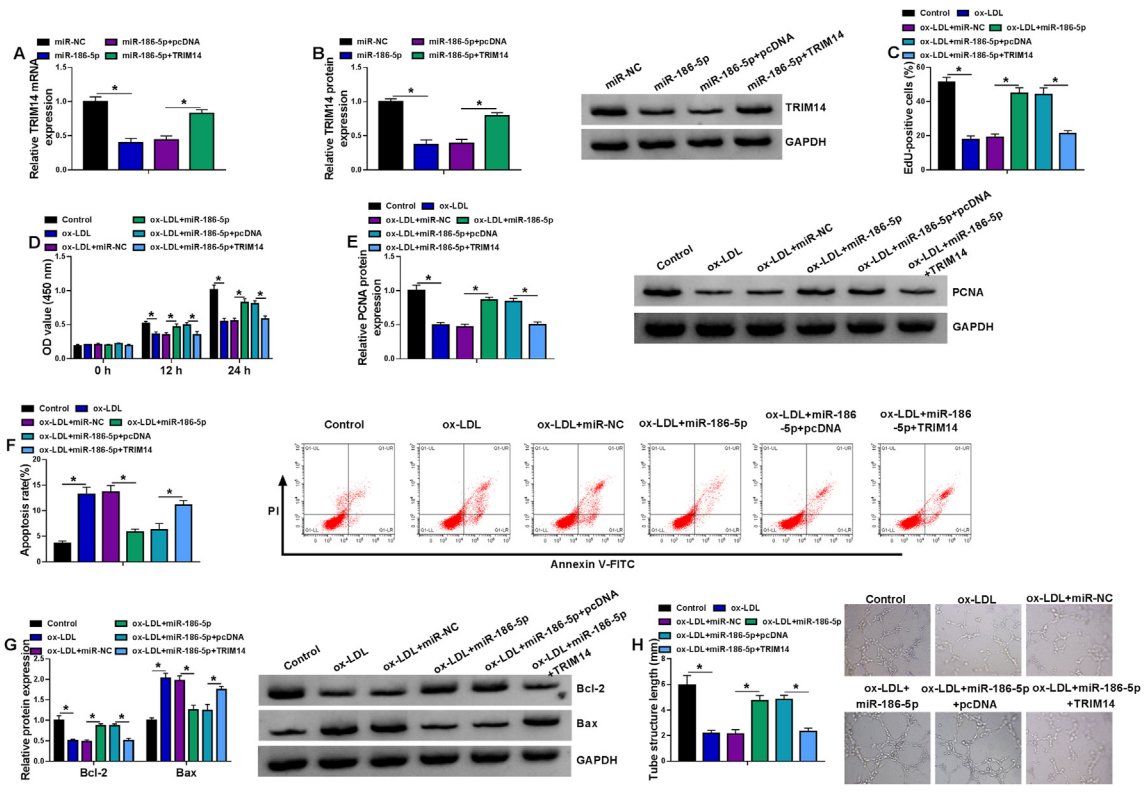

Fig. 6. MiR-186-5p overexpression alleviated ox-LDL-induced dysfunction in CMECs through targeting TRIM14. (A and B) The mRNA and protein levels of TRIM14 were analyzed by RT-qPCR and western blot assay in CMECs transfected with miR-NC, miR-186-5p, miR-186-5p + pcDNA, or miR-186-5p + TRIM14. (C–H) CMECs were divided into six groups: Control, ox-LDL, ox-LDL + miR-NC, ox-LDL + miR-186-5p, ox-LDL + miR-186-5p + pcDNA, and ox-LDL + miR-186-5p + TRIM14. (C and D) EdU assay and CCK-8 assay were used to detect cell proliferation ability. (E) Western blot assay was performed to apply analyze PCNA protein expression. (F) Cell apoptosis was detected by flow cytometry analysis. (G) The protein levels of Bcl-2 and Bax were analyzed using western blot assay. (H) The angiogenic ability was assessed using Matrigel tube formation assay. *$P < 0.05$.

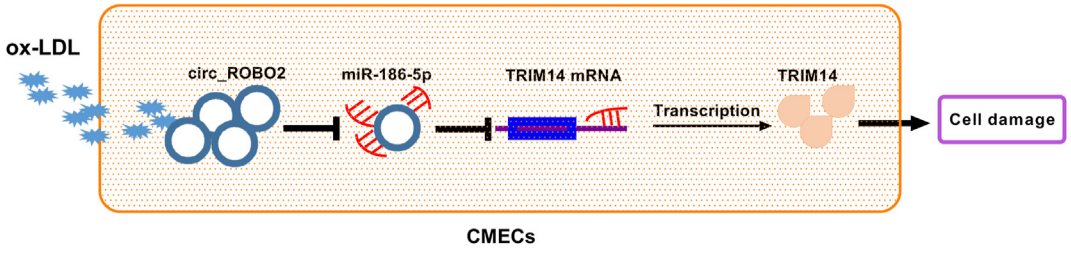

Fig. 7. Schematic diagram of the mechanism by which the circ_ROBO2/miR-186-5p/TRIM14 axis regulates ox-LDL-induced CMECs damage.

expression caused by sh-circ_ROBO2 were abrogated by down-regulating miR-186-5p in ox-LDL-exposed CMECs (Fig. 4F). In addition, the promoting effect of circ_ROBO2 silencing on angiogenesis was attenuated by miR-186-5p downregulation (Fig. 4G). These results indicated that circ_ROBO2 downregulation protected CMECs against ox-LDL-induced dysfunction partly through upregulating miR-186-5p.

3.5. TRIM14 was directly targeted by miR-186-5p

Many reports have shown that the roles of miRNAs are achieved by decreasing the expression of target mRNAs [23,24]. We used starBase to predict potential target genes of miR-186-5p. As displayed in Fig. 5A, the 3′UTR of TRIM14 contained the binding region with miR-186-5p, indicating that TRIM14 might be a target of miR-186-5p. The results of dual-luciferase reporter assay showed that miR-186-5p upregulation reduced the luciferase activity of TRIM14-WT, but did not affect the luciferase activity of TRIM14-MUT (Fig. 5B). Moreover, miR-186-5p was enriched by treatment with Bio-TRIM14-WT compared to Bio-TRIM14-MUT or Bio-NC groups (Fig. 5C). Transfection of miR-186-5p increased miR-186-5p expression and transfection of anti-miR-186-5p significantly decreased miR-186-5p expression (Fig. 5D), suggesting that miR-186-5p and anti-miR-186-5p were successfully transfected. Moreover, overexpression of miR-186-5p reduced TRIM14 mRNA and protein expression, while inhibition of miR-186-5p presented an opposite effect (Fig. 5E and F), indicating that TRIM14 was negatively regulated by miR-186-5p. In addition, TRIM14 mRNA expression was increased in serum of CAD patients and negative correlated with miR-186-5p expression as well as positive correlated with circ_ROBO2 expression in serum of CAD patients (Fig. 5G–I). Furthermore, TRIM14 mRNA and protein expression were both increased in CMECs treated with ox-LDL (Fig. 5J and K). Next, we explored whether circ_ROBO2 regulated TRIM14 expression via sponging miR-186-5p. As presented inFig. 5L and M, down-regulation of circ_ROBO2 led to the downregulation of TRIM14

mRNA and protein expression in CMECs, while co-transfection of sh-circ_ROBO2 and anti-miR-186-5p relieved this inhibition. Therefore, circ_ROBO2 modulated TRIM14 expression via interacting with miR-186-5p.

3.6. MiR-186-5p ameliorated ox-LDL-induced dysfunction in CMECs partly by regulating TRIM14

To explore whether miR-186-5p exerted its role in ox-LDL-induced CMECs via targeting TRIM14, rescue assays were performed. TRIM14 mRNA and protein levels were decreased by overexpression of miR-186-5p, while this inhibition was rescued by addition of TRIM14 (Fig. 6A and B). Overexpression of miR-186-5p increased DNA synthesis, cell viability, and PCNA protein expression, whereas these promotive effects were counteracted by upregulating TRIM14 (Fig. 6C-E), indicating miR-186-5p could abate the inhibitory effect of ox-LDL on proliferation by targeting TRIM14. In addition, cell apoptosis and Bax protein expression were reduced as well as Bcl-2 protein expression was enhanced by miR-186-5p upregulation, which could be neutralized by increasing TRIM14 expression (Fig. 6F and G), disclosing that miR-186-5p inhibited ox-LDL-induced apoptosis by downregulating TRIM14. Moreover, enforced expression of miR-186-5p neutralized the suppressive effect of ox-LDL on angiogenesis in CMECs, which was again reversed by accumulation of TRIM14 (Fig. 6H). Overall, miR-186-5p overexpression alleviated ox-LDL-induced damage in CMECs partly through reducing TRIM14 expression.

4. Discussion

CAD is mainly triggered by coronary atherosclerosis, and there is no effective and specific treatment strategy for CAD. Previous reports have shown that CAD is always accompanied by endothelial cell injury, which contributes to coronary atherosclerosis and aggravates the development of CAD [25]. Hence, uncovering the underlying mechanisms of CAD caused endothelial cell injury might help to treat CAD. Studies have shown that ox-LDL has a pivotal role in the pathogenesis and development of CAD by facilitating endothelial cell dysfunction [26]. Herein, we established CAD cell model was via exposing CMECs to ox-LDL. Moreover, we studied the role of circ_ROBO2 in CAD cell model and elucidated a novel ceRNA network of circ_ROBO2/miR-186-5p/TRIM14.

As a new kind of ncRNAs, circRNAs are involved in numerous pathophysiological processes in human diseases [27]. Previous researches have demonstrated that some circRNAs are dysregulated in CAD [28–31]. Circ_ROBO2 has been reported to promote ox-LDL-mediated endothelial injury in human vascular endothelial cells [32]. Moreover, circ_ROBO2 promoted hypoxia-induced cardiomyocytes damage via regulation of miR-590-3p/SOX4 axis [33]. In addition, circ_ROBO2 knockdown inhibited the proliferation and migration in PDGF-BB-treated human aortic smooth muscle cells [34]. These findings suggested that circ_ROBO2 played a pivotal role in cardiovascular diseases. Here, we observed that circ_ROBO2 was upregulated in serum samples of CAD patients, which was in line with previous study [14]. Moreover, we found that circ_ROBO2 was also overexpressed in ox-LDL-induced CMECs. Functional experiments presented that circ_ROBO2 downregulation alleviated ox-LDL-induced dysfunction in CMECs via promoting cell proliferation and angiogenesis and reducing apoptosis. Out results demonstrated that circ_ROBO2 downregulation might be a promising strategy for CAD treatment.

In general, as a ceRNA, the functions of circRNAs depend on the miRNA targets. We analyzed circ_ROBO2-miRNA interactions using circinteractome. We identified that miR-186-5p was a direct target of circ_ROBO2 after the online prediction and a series of analysis, and miR-186-5p was negatively regulated by circ_ROBO2. MiR-186-5p was reported to act as a tumor-suppressing or tumor-promoting miRNA in different malignancies via regulating the downstream genes and signal pathway [35–38]. In addition, Zhang et al. declared that SNHG7 sponged miR-186-5p to modulate endothelial cells' phenotype [20]. More importantly, Li et al. suggested that miR-186-5p exerted a protective role by downregulating ROBO1 in ox-LDL-exposed human umbilical vein endothelial cells [39]. Nevertheless, the function of miR-186-5p in CAD is still unclear. In this research, a low abundance of miR-186-5p was observed in CAD patient and ox-LDL-induced CMECs. Rescue experiments showed that miR-186-5p downregulation abated the protective role of sh-circ_ROBO2 in ox-LDL-induced dysfunction, disclosing that circ_ROBO2 might modulate the progression of CAD partly via targeting miR-186-5p.

MiRNAs can modulate gene expression via inhibiting translation or degrading target mRNAs [40]. Next, we further explored the possible targets for miR-186-5p. We proved that miR-186-5p directly targeted TRIM14. Moreover, circ_ROBO2 could positively regulate TRIM14 expression via interacting with miR-186-5p. TRIM14 has been identified as an oncogene many cancers [41–43]. Additionally, Huang et al. reported that TRIM14 could promote the activation of endothelium by regulating NF-κB signaling pathway [44]. Zhang et al. found that TRIM14 overexpression largely overturned the protective role of miR-328-3p in ox-LDL-triggered dysfunction in human umbilical vein endothelial cells [21]. Here, an upregulation of TRIM14 was observed in CAD patient and ox-LDL-exposed CMECs. To analyze whether miR-186-5p could regulate the biological phenotypes of CMECs through reducing TRIM14 expression, compensation experiments were performed. Our findings disclosed that miR-186-5p could protect CMECs against ox-LDL-induced injury partly via downregulating TRIM14. Despite these results, there are some limitations and shortcomings in the current study. First, the role of circ_ROBO2 in CAD disease causal pathways was not fully demonstrated in our study. Secondly, one gene may be targeted and regulated by multiple molecules; other circRNA/miRNAs might also contribute to the progression of CAD through regulating TRIM14. Third, the role of circ_ROBO2/miR-186-5p/TRIM14 in CAD is still required to be further confirmed in animal models in the future study.

In conclusion, circ_ROBO2 weakened ox-LDL-stimulated CMECs injury partly via sponging miR-186-5p and regulating TRIM14 (Fig. 7), indicating that inhibition of circ_ROBO2 might be a possible target for the treatment of CAD.

Funding

None.

Declaration of competing interest

The authors declare that they have no known competing financial interests or personal relationships that could have appeared to influence the work reported in this paper.

References

[1] Wong ND. Epidemiological studies of chd and the evolution of preventive cardiology. Nat Rev Cardiol 2014;11(5):276–89.
[2] Jung JH, Song GG, Kim JH, Seo YH, Choi SJ. Association of factor xiii val34leu polymorphism and coronary artery disease: a meta-analysis. Cardiol J 2017;24(1):74–84.
[3] Dalen JE, Alpert JS, Goldberg RJ, Weinstein RS. The epidemic of the 20(th) century: coronary heart disease. Am J Med 2014;127(9):807–12.
[4] Kandaswamy E, Zuo L. Recent advances in treatment of coronary artery disease: role of science and technology. Int J Mol Sci 2018;19(2):424.

[5] Di Pietro N, Formoso G, Pandolfi A. Physiology and pathophysiology of oxldl uptake by vascular wall cells in atherosclerosis. Vasc Pharmacol 2016;84:1–7.
[6] Gao W, Cui H, Li Q, Zhong H, Yu J, Li P, et al. Upregulation of microrna-218 reduces cardiac microvascular endothelial cells injury induced by coronary artery disease through the inhibition of hmgb1. J Cell Physiol 2020;235(3):3079–95.
[7] Liu J, Liu T, Wang X, He A. Circles reshaping the rna world: from waste to treasure. Mol Cancer 2017;16(1):58.
[8] Memczak S, Jens M, Elefsinioti A, Torti F, Krueger J, Rybak A, et al. Circular rnas are a large class of animal rnas with regulatory potency. Nature 2013;495(7441):333.
[9] Shang Q, Yang Z, Jia R, Ge S. The novel roles of circrnas in human cancer. Mol Cancer 2019;18(1):6.
[10] Zhang Z, Yang T, Xiao J. Circular rnas: promising biomarkers for human diseases. EBioMedicine 2018;34:267–74.
[11] Yu H, Zhao L, Zhao Y, Fei J, Zhang W. Circular rna circ_0029589 regulates proliferation, migration, invasion, and apoptosis in ox-ldl-stimulated vsmcs by regulating mir-424-5p/igf2 axis. Vasc Pharmacol 2020;135:106782.
[12] Li D, Jin W, Sun L, Wu J, Hu H, Ma L. Circ_0065149 alleviates oxidized low-density lipoprotein-induced apoptosis and inflammation in atherosclerosis by targeting mir-330-5p. Front Genet 2021;12:590633.
[13] Ji P, Song X, Lv Z. Knockdown of circ_0004104 alleviates oxidized low-density lipoprotein-induced vascular endothelial cell injury by regulating mir-100/tnfaip8 axis. J Cardiovasc Pharmacol 2021;78(2):269–79.
[14] Zhao Z, Li X, Gao C, Jian D, Hao P, Rao L, et al. Peripheral blood circular rna hsa_circ_0124644 can be used as a diagnostic biomarker of coronary artery disease. Sci Rep 2017;7:39918.
[15] Bach DH, Lee SK, Sood AK. Circular rnas in cancer. Mol Ther Nucleic Acids 2019;16:118–29.
[16] Panda AC. Circular rnas act as mirna sponges. Adv Exp Med Biol 2018;1087:67–79.
[17] Ardekani AM, Naeini MM. The role of micrornas in human diseases. Avicenna J Med Biotechnol (AJMB) 2010;2(4):161–79.
[18] Liu MN, Luo G, Gao WJ, Yang SJ, Zhou H. Mir-29 family: a potential therapeutic target for cardiovascular disease. Pharmacol Res 2021;166:105510.
[19] Zhang Q, Liu S, Zhang J, Ma X, Dong M, Sun B, et al. Roles and regulatory mechanisms of mir-30b in cancer, cardiovascular disease, and metabolic disorders (review). Exp Ther Med 2021;21(1):44.
[20] Zhang S, Zhu X, Li G. E2f1/snhg7/mir-186-5p/mmp2 axis modulates the proliferation and migration of vascular endothelial cell in atherosclerosis. Life Sci 2020;257:118013.
[21] Zhang C, Wang L, Shen Y. Circ_0004104 knockdown alleviates oxidized low-density lipoprotein-induced dysfunction in vascular endothelial cells through targeting mir-328-3p/trim14 axis in atherosclerosis. BMC Cardiovasc Disord 2021;21(1):207.
[22] Haque S, Harries LW. Circular rnas (circrnas) in health and disease. Genes 2017;8(12):353.
[23] Ni WJ, Leng XM. Mirna-dependent activation of mrna translation. MicroRNA 2016;5(2):83–6.
[24] Afonso-Grunz F, Müller S. Principles of mirna-mrna interactions: beyond sequence complementarity. Cell Mol Life Sci 2015;72(16):3127–41.
[25] Zhu Y, Zhang Y, Huang X, Xie Y, Qu Y, Long H, et al. Z-ligustilide protects vascular endothelial cells from oxidative stress and rescues high fat diet-induced atherosclerosis by activating multiple nrf2 downstream genes. Atherosclerosis 2019;284:110–20.
[26] Wang X, Li X, Wu Y, Song Y. Upregulation of mir-223 abrogates nlrp3 inflammasome-mediated pyroptosis to attenuate oxidized low-density lipoprotein (ox-ldl)-induced cell death in human vascular endothelial cells (ecs). In Vitro Cell Dev Biol Anim 2020;56(8):670–9.
[27] Zhang Y, Zhang X-O, Chen T, Xiang J-F, Yin Q-F, Xing Y-H, et al. Circular intronic long noncoding rnas. Mol Cell 2013;51(6):792–806.
[28] Liang B, Li M, Deng Q, Wang C, Rong J, He S, et al. Circrna znf609 in peripheral blood leukocytes acts as a protective factor and a potential biomarker for coronary artery disease. Ann Transl Med 2020;8(12):741.
[29] Miao L, Yin RX, Zhang QH, Liao PJ, Wang Y, Nie RJ, et al. A novel circrna-mirna-mrna network identifies circ-yod1 as a biomarker for coronary artery disease. Sci Rep 2019;9(1):18314.
[30] Pan RY, Zhao CH, Yuan JX, Zhang YJ, Jin JL, Gu MF, et al. Circular rna profile in coronary artery disease. Am J Transl Res 2019;11(11):7115–25.
[31] Wang L, Shen C, Wang Y, Zou T, Zhu H, Lu X, et al. Identification of circular rna hsa_circ_0001879 and hsa_circ_0004104 as novel biomarkers for coronary artery disease. Atherosclerosis 2019;286:88–96.
[32] Wang G, Li Y, Liu Z, Ma X, Li M, Lu Q, et al. Circular rna circ_0124644 exacerbates the ox-ldl-induced endothelial injury in human vascular endothelial cells through regulating papp-a by acting as a sponge of mir-149-5p. Mol Cell Biochem 2020;471(1–2):51–61.
[33] Tan J, Pan W, Chen H, Du Y, Jiang P, Zeng D, et al. Circ_0124644 serves as a cerna for mir-590-3p to promote hypoxia-induced cardiomyocytes injury via regulating sox4. Front Genet 2021;12:667724.
[34] Lin DS, Zhang CY, Li L, Ye GH, Jiang LP, Jin Q. Circ_robo2/mir-149 axis promotes the proliferation and migration of human aortic smooth muscle cells by activating nf-κb signaling. Cytogenet Genome Res 2021;161:414–24.
[35] Zhang Z, Zhang W, Mao J, Xu Z, Fan M. Mir-186-5p functions as a tumor suppressor in human osteosarcoma by targeting foxk1. Cell Physiol Biochem 2019;52(3):553–64.
[36] Li J, Xia L, Zhou Z, Zuo Z, Xu C, Song H, et al. Mir-186-5p upregulation inhibits proliferation, metastasis and epithelial-to-mesenchymal transition of colorectal cancer cell by targeting zeb1. Arch Biochem Biophys 2018;640:53–60.
[37] Islam F, Gopalan V, Vider J, Wahab R, Ebrahimi F, Lu CT, et al. Microrna-186-5p overexpression modulates colon cancer growth by repressing the expression of the fam134b tumour inhibitor. Exp Cell Res 2017;357(2):260–70.
[38] Feng H, Zhang Z, Qing X, French SW, Liu D. Mir-186-5p promotes cell growth, migration and invasion of lung adenocarcinoma by targeting pten. Exp Mol Pathol 2019;108:105–13.
[39] Li S, Huang T, Qin L, Yin L. Circ_0068087 silencing ameliorates oxidized low-density lipoprotein-induced dysfunction in vascular endothelial cells depending on mir-186-5p-mediated regulation of roundabout guidance receptor 1. Front Cardiovasc Med 2021;8:650374.
[40] Fabian MR, Sonenberg N, Filipowicz W. Regulation of mrna translation and stability by microrna. Annu Rev Biochem 2010;79:351–79.
[41] Jin Z, Li H, Hong X, Ying G, Lu X, Zhuang L, et al. Trim14 promotes colorectal cancer cell migration and invasion through the sphk1/stat3 pathway. Cancer Cell Int 2018;18:202.
[42] Wang F, Ruan L, Yang J, Zhao Q, Wei W. Trim14 promotes the migration and invasion of gastric cancer by regulating epithelial-to-mesenchymal transition via activation of akt signaling regulated by mir-195-5p. Oncol Rep 2018;40(6):3273–84.
[43] Shen W, Jin Z, Tong X, Wang H, Zhuang L, Lu X, et al. Trim14 promotes cell proliferation and inhibits apoptosis by suppressing pten in colorectal cancer. Cancer Manag Res 2019;11:5725–35.
[44] Huang X, Li Y, Li X, Fan D, Xin HB, Fu M. Trim14 promotes endothelial activation via activating nf-κb signaling pathway. J Mol Cell Biol 2020;12(3):176–89.